

AD-A140 718

SEM (SCANNING-ELECTRON-MICROSCOPY) STUDIES OF MAGNETIC 1/1
DOMAINS IN AMORPHO..(U) GENERAL ELECTRIC CORPORATE
RESEARCH AND DEVELOPMENT SCHENECTA.. J D LIVINGSTON

UNCLASSIFIED

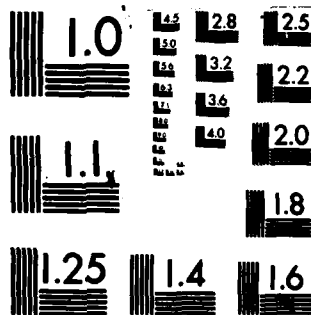
JAN 84 84-SRD-019 N00014-82-C-0060

F/G 11/6

NL



END
DATE
FORMED
16-84
DTIC



MICROCOPY RESOLUTION TEST CHART
NATIONAL BUREAU OF STANDARDS-1963-A

12

SEM STUDIES OF MAGNETIC DOMAINS IN AMORPHOUS METALS

AD-A140 718

Annual Report
Contract No. N00014-82-C-0060

Prepared for

Department of the Navy
Office of Naval Research
Arlington, Virginia 22217

Prepared by

Properties Branch
Metallurgy Laboratory
Corporate Research and Development
General Electric Company
Schenectady, New York 12301

January 1984

Reproduction in whole or in part is permitted for any
purpose of the United States Government

Approved for public release; distribution unlimited.

DTIC
ELECTE
MAY 3 1984
S B

FILE COPY

84-870-000

84 04 30 059

REPORT DOCUMENTATION PAGE

1a. REPORT SECURITY CLASSIFICATION unclassified		1b. RESTRICTIVE MARKINGS	
2a. SECURITY CLASSIFICATION AUTHORITY		3. DISTRIBUTION/AVAILABILITY OF REPORT Approved for public release; distribution unlimited.	
2b. DECLASSIFICATION/DOWNGRADING SCHEDULE			
4. PERFORMING ORGANIZATION REPORT NUMBER(S) 84 SRD 019		5. MONITORING ORGANIZATION REPORT NUMBER(S)	
6a. NAME OF PERFORMING ORGANIZATION General Electric Company Corporate Research and Development	6b. OFFICE SYMBOL <i>(If applicable)</i>	7a. NAME OF MONITORING ORGANIZATION	
6c. ADDRESS (City, State and ZIP Code) Schenectady, NY 12301		7b. ADDRESS (City, State and ZIP Code)	
8a. NAME OF FUNDING/SPONSORING ORGANIZATION Department of the Navy Office of Naval Research	8b. OFFICE SYMBOL <i>(If applicable)</i> Code 430	9. PROCUREMENT INSTRUMENT IDENTIFICATION NUMBER N00014-82-C-0060	
8c. ADDRESS (City, State and ZIP Code) Arlington, VA 22217		10. SOURCE OF FUNDING NOS.	
		PROGRAM ELEMENT NO.	PROJECT NO.
11. TITLE (Include Security Classification) SEM Studies of Magnetic Domains in Amorphous Metals			
12. PERSONAL AUTHOR(S) J.D. Livingston			
13a. TYPE OF REPORT Annual Report	13b. TIME COVERED FROM Dec 1982 TO Nov 1983	14. DATE OF REPORT (Yr., Mo., Day) January 1984	15. PAGE COUNT
16. SUPPLEMENTARY NOTATION			
17. COSATI CODES		18. SUBJECT TERMS (Continue on reverse if necessary and identify by block number)	
FIELD	GROUP	SUB. GR.	amorphous metals, magnetic domains, scanning electron microscopy magnetomechanical properties, magnetic anisotropy, magnetic properties
19. ABSTRACT (Continue on reverse if necessary and identify by block number) Magnetic domain structures in amorphous ribbons were characterized by SEM and Bitter technique. Studies included effects of anisotropy constant, applied currents, twisting, etc. Results were related to magnetic and magnetomechanical properties.			
20. DISTRIBUTION/AVAILABILITY OF ABSTRACT UNCLASSIFIED/UNLIMITED <input type="checkbox"/> SAME AS RPT. <input checked="" type="checkbox"/> DTIC USERS <input type="checkbox"/>		21. ABSTRACT SECURITY CLASSIFICATION unclassified	
22a. NAME OF RESPONSIBLE INDIVIDUAL D.E. Polk		22b. TELEPHONE NUMBER <i>(Include Area Code)</i> (202) 696-4402	22c. OFFICE SYMBOL Code 430

TABLE OF CONTENTS

Section		Page
1	BACKGROUND	1-1
	1.1 Amorphous Metals	1-1
	1.2 Anisotropy Types	1-1
	1.3 Pre-Contract Work	1-2
	1.4 First Year (12/81-11/82)	1-2
2	CONTRACT PROGRESS	2-1
	2.1 Effects of Anisotropy Constant	2-1
	2.2 Effects of Applied Currents	2-1
	2.3 Twisted Ribbons	2-2
	2.4 Other Studies	2-2
	2.5 Presentations and Interactions	2-3
3	REFERENCES	3-1
	APPENDIX A	A-1
	APPENDIX B	B-1

S **DTIC** **D**
ELECTE
 MAY 3 1984
B

Accession For	
NTIS GRA&I	<input checked="" type="checkbox"/>
DTIC TAB	<input type="checkbox"/>
Unannounced	<input type="checkbox"/>
Justification	
By _____	
Distribution/	
Availability Codes	
Dist	Avail and/or Special
A1	



Section 1 BACKGROUND

1.1 Amorphous Metals

Melt-spun ribbons of amorphous magnetic alloys, particularly alloys of transition metals such as Fe, Ni, and Co with metalloids such as B, Si, and C, have been under intensive study for several years. Their lack of grain structure and of magnetocrystalline anisotropy allows the attainment of excellent soft magnetic properties. In addition, they exhibit high mechanical strength and hardness and, in some cases, high corrosion resistance. As a result, these newly-available materials are being evaluated for various magnetic and magnetomechanical applications. Although their largest-volume application may eventually be as core materials in distribution transformers, in the near future they appear likely to be used primarily in high-frequency and electronic applications and as transducers and sensors, e.g., sonar sensors for the Navy. For some applications, amorphous alloys may be used in the form of sputtered films rather than melt-spun ribbons.

An important feature of amorphous magnetic alloys, not yet fully exploited, is that their technical magnetic properties can be varied over a wide range by variations in annealing and processing history. These variations produce different distributions of magnetic anisotropies and magnetic domain structures, resulting in variations in ac losses, permeability, coercivity, magnetostriction, etc. Magnetic domain structures are determined largely by the specimen shape and by the orientation, symmetry, and magnitude of the magnetic anisotropies present. In amorphous metals, these anisotropies usually result from magnetic annealing and/or from internal or applied stresses interacting with magnetostriction.

1.2 Anisotropy Types

For 60-Hz transformer applications, ribbons have usually been annealed in a longitudinal field to produce *longitudinal* anisotropy, i.e., a low-energy or "easy" magnetic axis along the ribbon length. This can produce high permeabilities, low coercivities, and square-loop magnetic behavior. Magnetization in longitudinal field occurs primarily by the motion of 180° domain walls. Eddy-current losses are proportional to the average domain width, which can be 1 mm or more, and losses may be nearly 100 times higher than classically-calculated eddy-current losses.

Transverse anisotropy, i.e., an easy axis parallel to the ribbon width, produces maximum magnetomechanical coupling and is therefore of interest for transducer and sensor applications. Magnetization in longitudinal field occurs primarily by rotation rather than by domain-wall motion. Eddy-current losses are low, approaching the classical limit, and hence transverse anisotropy is also of interest for high-frequency applications. However, magnetos-trictive length change is maximum, and the magnetic hysteresis loop is sheared, i.e., permeability is lowered.

Perpendicular anisotropy, with the easy axis normal to the ribbon plane, produces a very fine internal domain structure and a closure-domain structure at the surfaces. Magnetization in longitudinal fields will generally involve both rotation and domain-wall motion, yielding intermediate properties.

Easy-axis orientations between these three limiting cases, or *oblique* anisotropies, can also be produced. The resulting combination of properties may be favorable for particular applications.

1.3 Pre-Contract Work

Prior to the present contract, we had studied domain structures in amorphous metals by Bitter and scanning-electron-microscopy (SEM) techniques⁽¹⁻⁶⁾, in support of the General Electric development program for amorphous metal distribution transformers. Emphasis had been on ribbons with longitudinal anisotropy, although oblique in-plane anisotropy was also studied⁽⁵⁾.

We proposed in August 1981 to use our techniques to study anisotropy and domain control in amorphous metals. Special emphasis was placed on transverse and oblique anisotropies because of their importance in transducer and high-frequency applications. Domain observations were to be coupled with magnetomechanical measurements by A. E. Clark and co-workers at the Naval Surface Weapons Center (NSWC).

In preparation for the contract, a simplified model of the magnetomechanical properties of transverse-anisotropy ribbons was developed⁽⁷⁾. The treatment emphasizes the importance of a low and uniform anisotropy in producing high magnetomechanical coupling, and is similar to that independently developed by Spano et al⁽⁸⁾. Plans for specific domain experiments were developed after a visit to NSWC in November 1981.

1.4 First Year (12/81-11/82)

The major results of the first year's contract work have been published⁽⁹⁾. The work focussed on melt-spun, iron-rich amorphous ribbons annealed to produce transverse or oblique magnetic anisotropy, because such ribbons will be of importance in magnetostrictive transducer applications. The compositions studied included Allied 2605CO ($\text{Fe}_{67}\text{Co}_{18}\text{B}_{14}\text{Si}_1$), Allied 2605SC ($\text{Fe}_{81}\text{B}_{13.5}\text{Si}_{3.5}\text{C}_2$), and a General Electric-produced alloy ($\text{Fe}_{81}\text{B}_{15}\text{Si}_3\text{C}_1$). The major conclusions of this work were:

(1) Domains in transverse-anisotropy ribbons are much finer than in longitudinal-anisotropy ribbons because of the transverse demagnetizing factor. Domains are finer in narrow ribbons than in wide ones.

(2) Domains in a high-anisotropy alloy (2605CO) are straighter than in the lower-anisotropy 2605SC and GE alloys, in which domain curvature from residual or applied stresses and local demagnetizing fields can be severe.

(3) Domains are finer in the 2605CO ribbons than in the other ribbons, partly because the higher anisotropy constant K decreases the μ^* -effect on magnetostatic energy, and partly because of greater thickness.

(4) Application of a dc longitudinal field to transverse-anisotropy ribbons decreases domain contrast (because of magnetization rotation) and produces domain refinement. Some of this refinement is retained on removal of the field, leading to slightly finer domains after dc demagnetization than after ac demagnetization.

(5) Application of longitudinal tensile stresses to ribbons with transverse or oblique anisotropy produces domain rotation, which can be used to determine the anisotropy constant K. Domain rotation with increasing stress is more abrupt for transverse anisotropy than for oblique anisotropy.

Section 2 CONTRACT PROGRESS

2.1 Effects of Anisotropy Constant

One of the interesting results of the first year's work was the observation of an effect of anisotropy constant on domain width in transverse-anisotropy ribbons. This effect was observed by comparing ribbons of 2605CO and 2605SC. However, these ribbons also differed in other respects, such as ribbon thickness, surface roughness, etc. It was decided that this effect could be studied more quantitatively by using samples of one alloy annealed at different temperatures and times to produce different anisotropy constants.

The alloy chosen was $\text{Co}_{70.3}\text{Fe}_{4.7}\text{Si}_{15}\text{B}_{10}$, for which the kinetics of both the development of induced anisotropy and the reorientation of this anisotropy had been extensively studied by workers at the University of Pennsylvania⁽¹⁰⁻¹³⁾. This alloy is also well suited for anisotropy studies because it has near-zero magnetostriction and therefore magnetic anisotropy is relatively insensitive to residual and applied stresses. Comparison with earlier results on iron-rich ribbons can clarify the role of magnetostriction in the domain phenomena observed.

The major results of this work have been published⁽¹⁴⁾. Observations were made on a series of four ribbons annealed at different temperatures to produce transverse anisotropy constants, and also on a series of ribbons annealed first to produce longitudinal anisotropy and then for various times in transverse field to produce a reorientation of the anisotropy. The major conclusions of this study were:

(1) The average domain width after ac demagnetization was found to vary as $K_u^{-1/6}$, where K_u is the induced transverse anisotropy constant. This is consistent with the predictions of several theories incorporating the μ^* -effect, i.e., the deviation of the magnetization from the easy-axis direction along the ribbon edge.

(2) The refinement of transverse domains by dc longitudinal field observed in Fe-rich ribbons (reported earlier) was not observed in this Co-rich alloy with near-zero magnetostriction. This suggests that this earlier effect may have been associated with magnetostrictive contributions to the total energy of the domain structure.

(3) Ribbons of the second series, annealed just long enough to produce a transition from longitudinal to transverse anisotropy, contained domains considerably wider than those in the ribbon of the first series with the lowest anisotropy ($K_u \approx 140 \text{ erg/cm}^3$). This suggests that K_u in these samples was even lower. However, domain widths in these samples were irregular and varied substantially with time and magnetic history, and thus quantitative determinations of K_u were not possible.

(4) The transition from longitudinal to transverse domain structures occurred at a shorter annealing time than the maximum in initial permeability in longitudinal field. This indicates that initial permeability is higher for low transverse K_u than for $K_u = 0$, an effect we attributed to different dependences of permeability on K_u for rotation and for domain-wall processes.

2.2 Effects of Applied Currents

Several transducer and sensor applications have been suggested involving the passage of electric current down an amorphous ribbon. In addition, several fundamental papers have employed the effects of applied currents to measure fundamental materials parameters. We modified our sample holder for the SEM to allow the application of dc and/or ac currents to

amorphous ribbons, and have directly observed the effects of alternating and direct currents on domain structures in both transverse-anisotropy and longitudinal-anisotropy ribbons.

The major results of this study were organized into a report (Appendix A) that has been accepted for publication⁽¹⁵⁾. The transverse-anisotropy ribbons studied were the same $\text{Co}_{70.3}\text{Fe}_{4.7}\text{Si}_{15}\text{B}_{10}$ ribbons used for the earlier study of the effects of anisotropy constant. Current-induced domain-wall motion was characterized and used to measure domain-wall energy and exchange constant as a function of anisotropy constant. A number of longitudinal-anisotropy ribbons annealed to produce different values of anisotropy were also studied, and current-induced magnetization rotation was directly observed by SEM. This rotation also produced an increase in initial permeability, and the current to produce maximum initial permeability was found to be proportional to anisotropy constant. This current for peak permeability may thus become a useful measure of longitudinal anisotropy.

2.3 Twisted Ribbons

Several sensors have been reported based on twisted amorphous ribbons. The shear stress produced by torsion results in an oblique anisotropy, and the resulting coupling of transverse and longitudinal components of magnetization produces several interesting effects. Longitudinal magnetic field can produce voltages along the ribbon (Matteucci effect) and applied currents can produce changes in longitudinal magnetization (inverse Wiedemann effect).

We have studied domain structures on twisted ribbons using the Bitter technique. In addition, several ribbons were given a stress-relief anneal while twisted. After cooling to room temperature, these ribbons were elastically untwisted, and the resulting domain structures were studied by Bitter and SEM techniques. In the SEM, the effects of applied fields and currents on domain structures in these untwisted ribbons were directly observed.

The results of this study will be presented at the 1984 Intermag Conference in Hamburg. An abstract of this paper is included as Appendix B. One major observation is the curvature of the domains across the ribbon width, indicating a departure from the pure shear stress state usually assumed for twisted ribbons. The curvatures found have been quantitatively correlated with the presence of longitudinal tensile and compressive stresses that result from second-order elastic effects. Other observations include the common presence of zig-zag domain walls (commonly observed only in thin films), a strong dependence of domain patterns on magnetic history, and the effects of applied currents and fields on domain-wall motion.

2.4 Other Studies

Several other studies pertaining to domains in amorphous ribbons have been undertaken but not yet brought to satisfactory completion. It is planned to complete these studies in 1984. Results of these partly-completed studies include:

Sputtered Films: A series of sputtered amorphous films have been studied by SEM. In several cases, transverse domain structures were observed in as-sputtered films, presumably reflecting a transverse anisotropy produced by a small transverse magnetic field present during sputtering. It is hoped to correlate various domain observations with such variables as film composition, film thickness, substrate material, sputtering and annealing conditions.

Bonding Stresses: Amorphous ribbons bonded to metal substrates with adhesives have been shown to possess domain structures indicating the presence of biaxial compressive stresses produced by the adhesive. These samples were obtained from the Naval Surface Weapons Center. Further studies to characterize the stresses produced by different adhesives are planned. These observations are pertinent to sensor and transducer designs requiring

bonding to a substrate, since the anisotropies produced by bonding stresses will alter magnetic and magnetomechanical properties.

Effects of Partial Crystallization: Several alloy heat treatments designed to optimize high-frequency magnetic properties apparently produce partial crystallization of the amorphous ribbons. We have observed domain structures in such ribbons and found evidence of transverse and perpendicular magnetic anisotropies, probably resulting from internal stresses produced by crystallization. These effects will be further characterized, with the goal of improved understanding of the effect of heat treatments on high-frequency permeability and losses.

2.5 Presentations and Interactions

Papers describing work done under this contract have been presented at the 1982 Intermag-3M Conference in Montreal, the 1983 Intermag Conference in Philadelphia, and the 1983 3M Conference in Pittsburgh. A paper on domains in twisted amorphous ribbons will be presented at the 1984 Intermag Conference in Hamburg. In addition, an overview of domain behavior in amorphous metals was presented at the Naval Research Laboratory in January 1983.

Interaction has been maintained with the magnetics group at the Naval Surface Weapons Center (NSWC). Howard Savage of that group visited our laboratories in October 1982 to present a seminar on transducer applications of amorphous metals, and met with General Electric sonar engineers. J. D. Livingston visited NSWC in January 1983 in conjunction with the NRL visit mentioned above. Samples studied on this contract have included samples provided by NSWC and samples provided by T. Jagielinski of the University of Pennsylvania. Jagielinski, who is being supported by a separate ONR contract, was a co-author on two recent papers^(14,15) and continues to cooperate closely with us. Technical interaction has also been maintained with other U.S., Japanese, and German scientists and engineers interested in transducer applications of amorphous metals.

Section 3
REFERENCES

1. Livingston, J.D., "Stresses and Magnetic Domains in Amorphous Metal Ribbons," *Phys. Stat. Sol. (a)* 56, 637 (1979).
2. Walter, J.L., Livingston, J.D., and Davis, A.M., "Cast-In Crystals in Amorphous Ribbons," *Mater. Sci. Eng.* 49, 47 (1981).
3. Livingston, J.D., and Morris, W.G., "SEM Studies of Magnetic Domains in Amorphous Ribbons," *IEEE Trans. Magn. MAG-17*, 2624 (1981).
4. Fiedler, H.C., Livingston, J.D., and Huang, S.C., "The Deleterious Effect of Aluminum in Fe-B-Si-C Amorphous Ribbon," *J. Magn. Magn. Mater.* 26, 157 (1982).
5. Luborsky, F.E., and Livingston, J.D., "Effect of Annealing Angle on the Magnetic Properties of an Amorphous Fe-B-Si-C Alloy," *IEEE Trans. Magn. MAG-18*, 908 (1982).
6. Huang, S.C., Frischmann, P.G., Luborsky, F.E., Livingston, J.D., and Mogro-Campero, A., "Effects of Ribbon Thickness and Annealing Temperature on the AC Magnetic Properties of the $Fe_{81.5}B_{14.5}Si_3C_1$ Alloy," *Rapidly-Solidified Amorphous and Crystalline Alloys*, 211, B.H. Kear, B.C. Giessen, and M. Cohen, eds., Elsevier, New York (1982).
7. Livingston, J.D., "Magnetomechanical Properties of Amorphous Metals," *Phys. Stat. Sol. (a)* 70, 591 (1982).
8. Spano, M.L., Hathaway, K.B., and Savage, H.T., "Magnetostriction and Magnetic Anisotropy of Field Annealed Metglas 2605 Alloys via dc M-H Loop Measurements Under Stress," *J. Appl. Phys.* 53, 2667 (1982).
9. Livingston, J.D., Morris, W.G., and Luborsky, F.E., "Domain Studies on Amorphous Ribbons with Transverse or Oblique Magnetic Anisotropy," 1982 Intermag Conference, *J. Appl. Phys.* 53, 7837 (1982).
10. Ho, K-Y, Flanders, P.J., and Graham, C.D. Jr., "Kinetics of Formation of Zero-Magnetostriction Amorphous Alloy," *J. Appl. Phys.* 53, 2279 (1982).
11. Ho, K-Y, "Isotropic Behavior of the Kinetics of Reorientation in an Amorphous Alloy," *J. Appl. Phys.* 53, 7828 (1982).
12. Jagielinski, T., "Elimination of Disaccommodation in Zero-Magnetostrictive FeCoSiB Amorphous Alloys," *J. Appl. Phys.* 53, 7852 (1982).
13. Jagielinski, T., "Kinetics of Changes in Initial Permeability Produced by Magnetic Annealing in a Zero-Magnetostrictive FeCoSiB Amorphous Alloy," *J. Appl. Phys.* 53, 7855 (1982).
14. Livingston, J.D., Morris, W.G., and Jagielinski, T., "Effects of Anisotropy on Domain Structures in Amorphous Ribbons," *IEEE Trans. Magn. MAG-19*, 1916 (1983).
15. Livingston, J.D., Morris, W.G., and Jagielinski, T., "Effects of Applied Currents on Domain Structures and Permeability in Amorphous Metal Ribbons," *J. Appl. Phys.* 55, (1984). (See Appendix A.)

Appendix A
EFFECTS OF APPLIED CURRENTS ON DOMAIN STRUCTURES
AND PERMEABILITY IN AMORPHOUS METAL RIBBONS

Introduction

The effects of applied currents on the magnetic properties and domain structures of amorphous metal ribbons are of both scientific⁽¹⁻⁴⁾ and technological⁽⁵⁾ interest. These effects depend upon the orientation and magnitude of the magnetic anisotropies in the ribbon.

Except in the immediate vicinity of the ribbon edge, the field produced by an applied current I is essentially transverse and varies linearly with distance from the ribbon midplane, reaching $I/2w$ at the ribbon surface, where w is the ribbon width. This field is oppositely directed on opposite faces of the ribbon. When the initial magnetic anisotropy and resulting domain structure are transverse (Figure 1a), this field therefore displaces domain walls in opposite directions on the opposite surfaces, producing curved domain walls (Figure 1b). Above a critical value of current, these curved walls are no longer stable, and a single wall centered on the ribbon midplane is produced (Figure 1e).

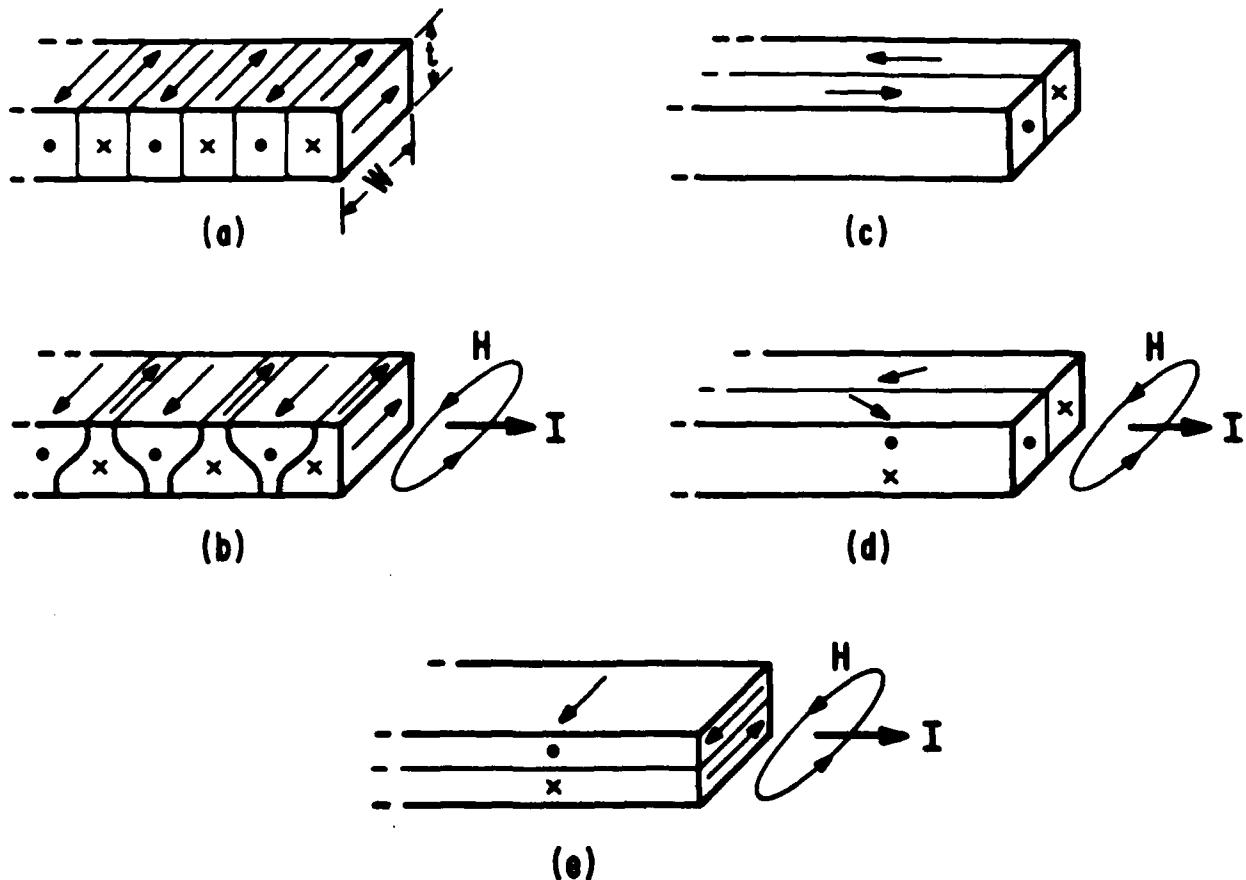


Figure A-1. Effect of applied current I on magnetization in amorphous metal ribbons (schematic). Transverse-anisotropy ribbon (a) without current and (b) with current. Longitudinal-anisotropy ribbon (c) without current and (d) with current. With sufficiently high current, both ribbons reach domain structure in (e).

This effect was analyzed by Williams and Shockley⁽⁶⁾ and Néel,⁽⁷⁾ and more recently by Hsu and Berger⁽³⁾ and Lopez, Aroca and Sanchez.⁽¹⁾ Assuming the domain-wall surface energy γ to be isotropic, the critical current I_c at which the curved walls disappear and the surface magnetization is saturated is given by

$$I_c = 4\gamma w / J_s t \quad (1)$$

where J_s is the saturation polarization and t is the ribbon thickness. For $I < I_c$, the wall displacement x is linear with current and given by

$$x = tI / 3I_c = t^2 J_s I / 12\gamma w \quad (2)$$

Higher-order terms in $x(I)$ are given by Néel.⁽⁷⁾ Either of these equations, or fitting to the full $x(I)$ curve,⁽¹⁾ can be used to measure domain-wall energy γ .

When the initial magnetic anisotropy and domain structures are instead longitudinal (Figure 1c), the transverse field produced by the current will induce a rotation of the magnetization that varies across the thickness of the ribbon (Figure 1d). At sufficiently high currents, the structure of Figure 1e will again be approached. Neglecting exchange and demagnetizing effects, the magnetization at the ribbon surface will rotate completely from longitudinal to transverse when the surface field equals the anisotropy field, i.e., when

$$I / 2w = 2K_u / J_s \quad (3)$$

where K_u is the uniaxial anisotropy constant. If this rotation were detectable, it could be used as a measure of K_u .

Experimental

The alloy studied was $\text{Co}_{70.3}\text{Fe}_{4.7}\text{Si}_{15}\text{B}_{10}$, an alloy of low magnetostriction ($\lambda_s = 2 \times 10^{-7}$) for which the development of magnetic anisotropy at various temperatures has been well documented.⁽⁸⁾ Melt-spun ribbon about 0.11 cm wide and 32 μm thick was cut into 5 cm lengths and annealed in a transverse field of 9 kOe or a longitudinal field of 220 Oe at various temperatures to produce a range of anisotropy constants.

Magnetic domain structures on the air (shiny) surfaces of the ribbons were studied in a JEOL 200 kV SEM. The sample holder used in previous studies of transverse-anisotropy ribbons^(9,10) was modified to allow the passage of alternating or direct currents through the sample. Dynamic studies of domain-wall motion were made using ac frequencies of about 58 Hz.

Longitudinal initial permeability was measured using an 0.2 mOe, 5 kHz field. This provided a direct measure of K_u for the transverse-anisotropy ribbons,⁽⁸⁾ and K_u for the longitudinal-anisotropy ribbons was obtained by assuming the same annealing kinetics. The effect of applied direct currents on initial permeability was studied for the longitudinal-anisotropy ribbons, which were immersed in water to limit Joule heating.

Results

Transverse-Anisotropy Ribbons

Alternating currents applied to these ribbons yield domain-wall oscillations that are directly revealed by the serrated wall images produced by the SEM (Figure 2). These serrated wall images result from the beating between the 58 Hz wall oscillations and the 60 Hz line scan of the SEM.⁽¹¹⁾ Variation in the amplitude of wall motion from wall to wall is apparent, and probably results from sample inhomogeneity. Wall motion can also be seen to vary along a given wall, and usually was greatest along the ribbon edge (which was slightly to the right of this figure). Data for determining wall energy were generally taken well away from the edge.



Figure A-2. Domain-wall motion in ribbon with transverse anisotropy constant $K_u = 195 \text{ J/m}^3$ produced by 58 Hz current of 21.3 ma (rms). Arrows indicate $100 \mu\text{m}$. Depth of serrations of wall images indicates amplitude of wall motion.

The variation of wall displacement with current could also be measured from static images taken at different values of direct current; results were in agreement with the ac results, provided a decreasing ac signal was first applied to reduce hysteretic effects.⁽¹⁾

At low currents, wall displacement is nearly linear with current, and the serrations appeared nearly sinusoidal. At higher currents, the nonlinear variation of displacement with current became apparent from the cusping of the serrations, as seen in Figure 2. For the sample shown, a slight increase in rms current amplitude to 22 ma produced a merging of neighboring serrations, i.e., saturation of the surface magnetization (Figure 1e). Thus the peak current (31 ma) had reached the critical current I_c given by Equation 1. Using $J_s = 0.67 T$, this yields a domain-wall energy for this ribbon of $1.5 \times 10^{-4} \text{ J/m}^2$ (0.15 ergs/cm²). An attempt was also made to calculate γ from measurements of wall displacements at small currents and Equation 2. However, the variation of displacement from wall to wall was much greater than at large currents, probably because of variations in wall pinning by defects. It was therefore decided that Equation 1 was a more satisfactory measure of γ . Similar measurements were made on three other ribbons annealed in transverse field at higher temperatures to produce lower values of K_u . A monotonic decrease of I_c (and therefore γ) with decreasing K_u was found, as seen in Table 1. Values of the exchange constant A were also calculated for each ribbon from the relationship $\gamma = 4(AK_u)^{1/2}$.

Table 1
DATA FOR TRANSVERSE-ANISOTROPY RIBBONS

Annealing Temperature (°C)	Transverse Anisotropy K_u (J/m^3)	Critical Current I_c (ma)	Domain-Wall Surface Energy ($10^{-4} J/m^2$)	Exchange Constant ($10^{-12} J/m$)
225	195	31	1.5	7.3
310	115	21	1.0	5.7
350	58	13	0.63	4.3
390	≈14	5.9	0.29	3.8

Longitudinal-Anisotropy Ribbons

The current-induced rotation of surface magnetization (Figure 1d) could be directly demonstrated by orienting ribbon in the SEM so that magnetic contrast was produced only by the transverse component of magnetization. An alternating current of about 58 Hz then produced periodic variations in intensity across the SEM image resulting from beating between the 58 Hz cyclic rotation of surface magnetization and the 60 Hz line scan. The contrast between neighboring intensity bands increased with increasing current, and for a given current was greater for ribbons with lower K_u , as expected. However, it was difficult to convert this contrast into a quantitative measure of rotation. Furthermore, for all but very small K_u values, the currents required to produce large magnetization rotation also produced significant heating of the ribbon in the vacuum environment of the SEM.

Instead, initial permeability measurements on ribbons immersed in water were found to produce a useful measure of magnetization rotation. Initial longitudinal permeability was measured as a function of applied direct current, and was found to increase and then decrease with increasing current. The current I_{max} that produced maximum permeability was proportional to the longitudinal anisotropy constant K_u (Figure 3). This current was about 50% higher than the current expected to produce full rotation of the surface magnetization through Equation 3.

Discussion

Current-induced wall motion in transverse-anisotropy ribbons (Figure 1b) and current-induced magnetization rotation in longitudinal-anisotropy ribbons (Figure 1d) have been directly observed by SEM.

In the former case, the limiting current I_c for wall stability was used to determine the domain-wall surface energy γ through Equation 1. The values obtained were all lower than the value of $4 \times 10^{-4} J/m^2$ measured by Dong and Kronmuller⁽¹²⁾ in an as-quenched alloy of similar composition using a different technique. The variation of domain-wall energy with anisotropy constant was somewhat greater than $K_u^{1/2}$, leading to a variation of exchange constant A with anisotropy. Using the same technique on a different amorphous alloy, Lopez, Aroca and Sanchez⁽¹⁾ also found a variation of A with anisotropy constant.

For longitudinal-anisotropy ribbons, the increase in initial permeability with applied current is consistent with earlier observations⁽⁸⁾ that, for a given K_u , longitudinal initial permeability was higher for transverse than for longitudinal anisotropy. The magnetization rotation produced by current (Figure 1d) brings more of the ribbon volume into the transverse magnetization orientation favorable for initial permeability. Peak permeability occurred at a current that produced a surface field about 50% higher than the anisotropy field. At this current, the outer third of the ribbon would be expected to be fully rotated, with the inner two-thirds of the ribbon only partially rotated. Although this technique appears to be a reliable means

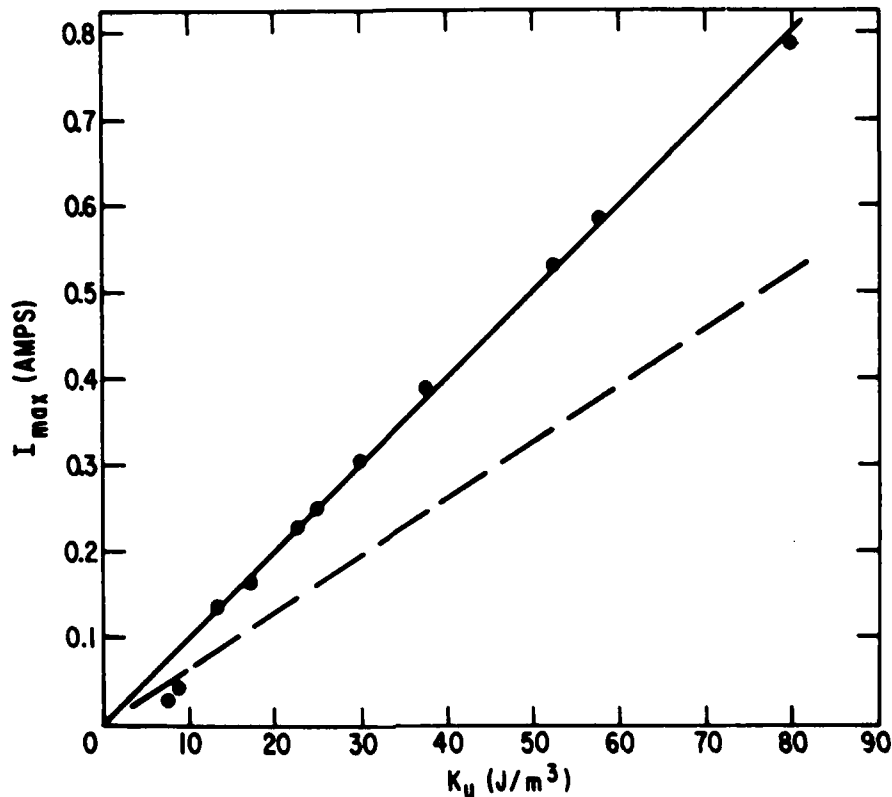


Figure A-3. Current I_{max} that produced maximum initial permeability vs. longitudinal anisotropy constant K_u . Dashed line shows current to produce full magnetization rotation at ribbon surface, given by Equation 3.

for determining K_u , extension to other alloys would require verification that a similar configuration would yield maximum initial permeability.

Acknowledgments

The amorphous ribbon was produced by H.H. Liebermann, and the work was partly supported by ONR.

References

1. Lopez, E., Aroca, C., and Sanchez, P., *J. Magn. and Magn. Matls.* 36, 175 (1983).
2. Aroca, C., Lopez, E., and Sanchez, P. *J. Magn. and Magn. Matls.* 23, 193 (1981).
3. Hsu, Y. and Berger, L., *J. Appl. Phys.* 53, 7873 (1982).
4. Nielsen, O.V., *J. Magn. and Magn. Matls.* 24, 81 (1981).
5. Dalpadado, R.N.G., *IEEE Trans. Magn. MAG-18*, 1785 (1982) and references therein.
6. Williams, H.J. and Shockley, W., *Phys. Rev.* 75, 178 (1949).
7. Néel, L., *Compt. Rend.* 254, 2891 (1963).
8. Jagielinski, T. *J. Appl. Phys.* 53, 7855 (1982) and references therein.
9. Livingston, J.D., Morris, W.G., and Luborsky, F.E., *J. Appl. Phys.* 53, 7837 (1982).
10. Livingston, J.D., Morris, W.G., and Jagielinski, T., *IEEE Trans. Magn. MAG-19*, 1916 (1983).
11. Livingston, J.D. and Morris, W.G., *IEEE Trans. Magn. MAG-17*, 2624 (1981).
12. Dong, X.Z. and Kronmuller, H., *Phys. Stat. Sol. (a)* 70, 451 (1982).

Appendix B MAGNETIC DOMAINS IN TWISTED AMORPHOUS RIBBONS

Introduction

The magnetic anisotropies and domain structures of Fe-rich amorphous alloy ribbons are very sensitive to stresses. The complex stress distribution in twisted amorphous ribbons produces a complex anisotropy distribution that leads to unusual magnetic behavior of both scientific^(1,2) and technological^(3,4) interest. To help understand this behavior, we have made direct observations of magnetic domain structures in twisted amorphous ribbons with SEM and Bitter techniques.

Results

Our SEM observations have been made using a sample holder that allows insitu application of dc and/or ac fields or currents to the sample as well as tilting and rotation of the sample to optimize magnetic contrast. Ribbon samples were given a stress-relief anneal after twisting. Thus when straightened to view in the SEM, they were stressed in elastic torsion.

The stress state in twisted ribbons has sometimes been assumed to be pure shear, which would produce a magnetic easy axis at $\pm 45^\circ$ to the specimen length (of opposite sign on opposite faces). However, a more detailed analysis indicates the additional presence of longitudinal tensile or compressive stresses that vary across the width of the ribbon. As a result, the orientation of the easy axis will vary across the ribbon width. This variation can be seen in the curvature of 180° walls when they extend across the ribbon width (Fig. 1a). In this case of elastic untwisting, longitudinal compression forces increase near the ribbon edges, rotating the easy axis (and the 180° domain walls) towards the transverse direction near the edges. The resulting angle at any location is a measure of the relative magnitude of the local shear and compressive stresses.

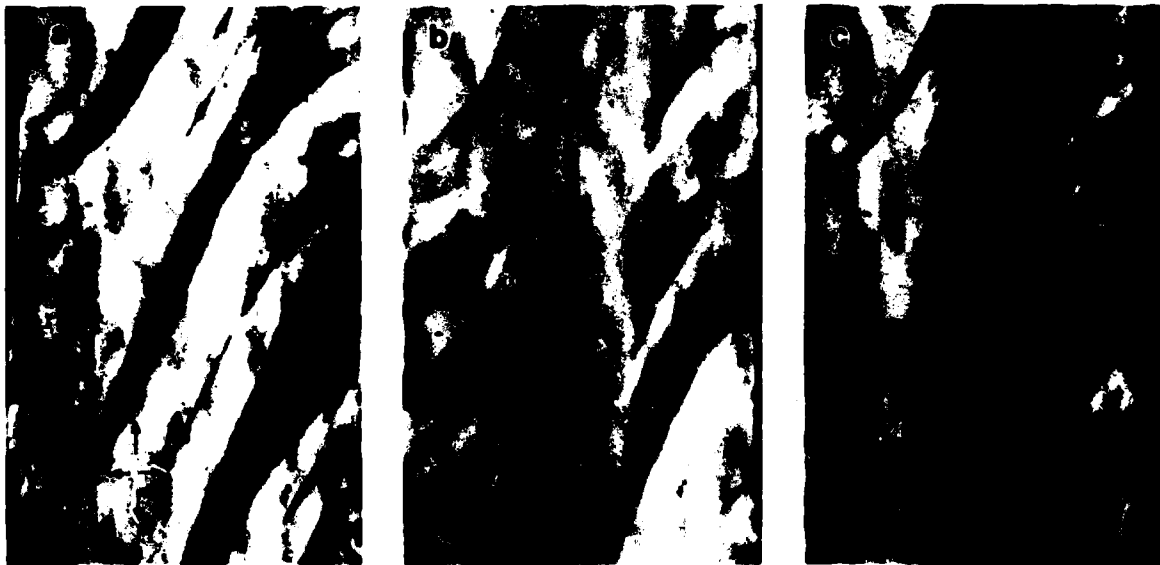


Figure B-1. SEM images of these unusual domain structures with applied field and currents have been characterized. SEM observations on elastically untwisted ribbon have been supplemented by Bitter observations on both elastically untwisted and elastically twisted ribbons. Results are interpreted in terms of the anisotropy gradients that occur both across the ribbon width and through the ribbon thickness.

Magnetic domain structures were found to be very sensitive to magnetic history. Figures 1b and 1c show domain structures in the same region shown in Figure 1a after different demagnetizing sequences. Figure 1c shows a longitudinal "zigzag" or "sawtooth" domain wall. Such charged walls are not usually seen in amorphous ribbons, but are commonly observed in magnetic thin films. We believe they occur in twisted ribbons because of the variation of anisotropy and domain structure through the ribbon thickness. Probably a longitudinal zigzag wall of opposite polarity is present on the opposite surface, thereby reducing magnetostatic energy.

The variation of these unusual domain structures with applied field and domain currents have been characterized. SEM observations on elastically untwisted ribbon have been supplemented by Bitter observations on both elastically untwisted and elastically twisted ribbons. Results are interpreted in terms of the anisotropy gradients that occur both across the ribbon width and through the ribbon thickness.

This work was supported in part by ONR.

References

1. Hernando, A., and Barandiaran, J.M., *Phys. Rev. B* 22, 2445, (1980).
2. Nielsen, O.V., *J. Magn. Mats.* 24, 81, (1981).
3. Mohri, K., and Takeuchi, S., *J. Appl. Phys.* 53, 8386, (1982).
4. Dalpadado, R.N.G., *IEEE Trans. Magn.* MAG-19, 2027, (1983).

**DAT
FILM**

